

# Large-scale synthesis of AgNWs with ultra-high aspect ratio above 4000 and their application in conductive thin film

Yongyun Mao<sup>1</sup> · Hongwei Yang<sup>1</sup> · Changyi Hu<sup>1</sup> · Junmei Guo<sup>1</sup> · Xianwei Meng<sup>1</sup> · Yuwen Yang<sup>1</sup>

Received: 14 September 2016 / Accepted: 5 December 2016 / Published online: 12 December 2016  
© Springer Science+Business Media New York 2016

**Abstract** Large-scale, uniform silver nanowires (AgNWs) with diameter of 30 nm and ultra-high aspect ratio up to 4000 were obtained by adding  $\text{Cu}^{2+}$  and  $\text{Fe}^{3+}$  to the AgNWs synthesis. AgNWs were longer at higher concentration of  $\text{Cu}^{2+}$  and better uniformity in the presence of both  $\text{Fe}^{3+}$  and  $\text{Cu}^{2+}$ . Finding indicate that by simply controlling  $\text{Cu}^{2+}/\text{Fe}^{3+}$  molar ratios in the reaction process, the high yield (98%), ultra-high aspect ratio (over 4000) and large-scale (over 50 g per pot) production of AgNWs can be obtained. Additionally, embedding the ultra-high aspect ratio AgNWs into polyvinyl alcohol (PVA) matrices, novel AgNWs@PVA flexible transparent conductor films (TCFs) with high-electrical conductivity performance was fabricated. This method improved the production efficiency of ultra-high aspect ratio AgNWs and could be applied to high performance TCFs; thus having major commercial implications.

## 1 Introduction

Flexible transparent conductor films (TCFs) enable today's ubiquitous flat panel displays and large-area touch screens, as well as numerous emerging applications such as light emitting diodes, thin-film solar cells, e-paper, sensor and electrostatic shielding [1–7]. Across all application areas, two critical performance criteria for TCFs are the optical transmittance (%T) and sheet resistance ( $R_s$ ). Fortunately,

silver nanowires (AgNWs) have attracted much attention for use in TCFs due to its high transmittance, low sheet resistances and flexibility [6]. In fact, the performance of AgNWs-based TCFs generally increases with decreasing diameter and increasing AgNWs aspect ratio due to the fact that thin AgNWs scatter less light, and increasing aspect ratio decreases the number of high-resistance wire–wire contacts in the film [8]. Also, it has been reported that TCFs fabricated with longer AgNWs could achieve a higher electrical conductivity since more inter-nanowires junctions improved the number of conductive paths compared to the shorter ones [9, 10]. More importantly, because of strong effect of nanowires diameter on their scattering efficiency, it has often been hypothesized that nanowires networks with longer length and smaller diameters will transmit more light at a given sheet resistance than films of nanowires with larger diameter [11]. Some conclusions have suggested that the length and diameter of the wires are critical factors for enabling the high transparency with a low haze, high electrical conductivity. This is because long wires with small diameters can form a more effective network with smaller wire number density by providing longer percolation paths and reducing the inter-nanowire junctions where the major contact resistant drop occurs. Therefore, extending the length of wires and keeping the diameter as low as possible are simple solution processes that have been a great challenge in the field of AgNWs applications on a large scale.

To meet the large demand of AgNWs, especially the ultra-long AgNWs, a large scale and stable synthesis method of AgNWs is needed. Up to present, the polyol process has been the most promising method for preparing AgNWs by using PVP as the capping agent and ethylene glycol (EG) as the solvent and reducing agent to reduce  $\text{AgNO}_3$  into AgNWs [12–15]. In the polyol process, many

✉ Yongyun Mao  
maoyongyun123@126.com

<sup>1</sup> State Key Laboratory of Advanced Technologies for Comprehensive Utilization of Platinum Metals, Kunming Institute of Precious Metals, Kunming, China

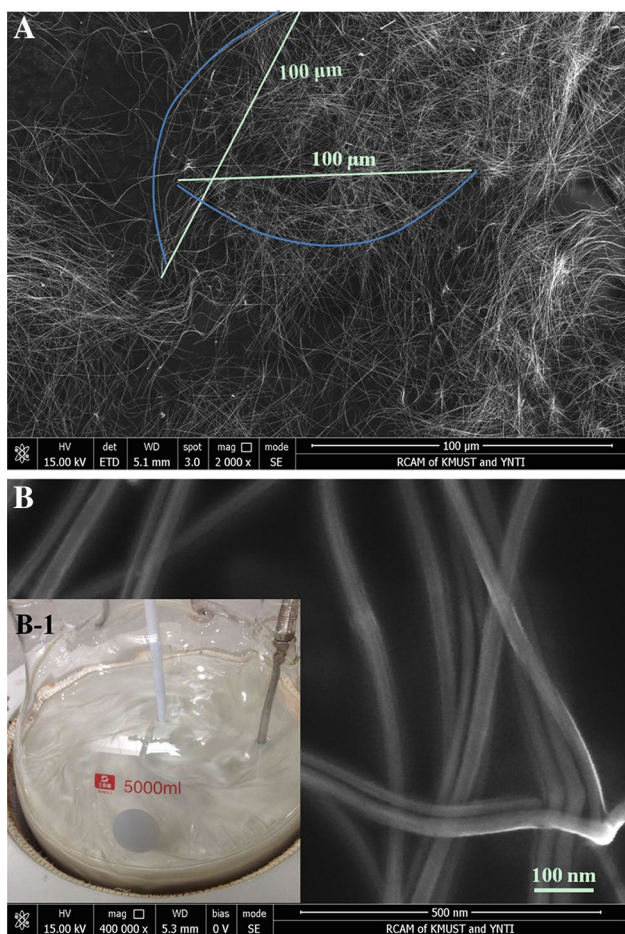


**Fig. 1** a, b SEM for the AgNWs prepared under  $\text{Cu}^{2+}/\text{Fe}^{3+}$  molar ratio of 5:2; b-1 digital photograph of large-scale synthesis of AgNWs

factors such as additive agents, temperature, stirring speed, reaction times, metal ions, and injection speed of chemicals have always affected the yield and morphology of AgNWs [16–21]. However, few researches on the large-scale (over 50 g per pot), uniform AgNWs with diameter of 30 nm and ultra-high aspect ratio up to 4000 were synthesized by simply controlling  $\text{Cu}^{2+}/\text{Fe}^{3+}$  molar ratios in the reaction process have been reported thus far.

Herein, a modified polyol synthesis method was used to produce uniform and ultra-high aspect ratio AgNWs by adjusting the different molar ratios of  $\text{Cu}^{2+}$  and  $\text{Fe}^{3+}$ . The results indicated that the  $\text{Cu}^{2+}/\text{Fe}^{3+}$  molar ratios could effectively change the morphology of AgNWs. In particular, AgNWs with good uniformity and ultra-high aspect ratio have been synthesized on a large scale under the optimized parameter of  $\text{Cu}^{2+}/\text{Fe}^{3+}$  molar ratios. As compared to the previous reports, the present method creates a fast and efficient executable method process for the synthesis of AgNWs with ultra-high aspect ratio at a large scale. More importantly, ultra-high aspect ratio AgNWs with longer

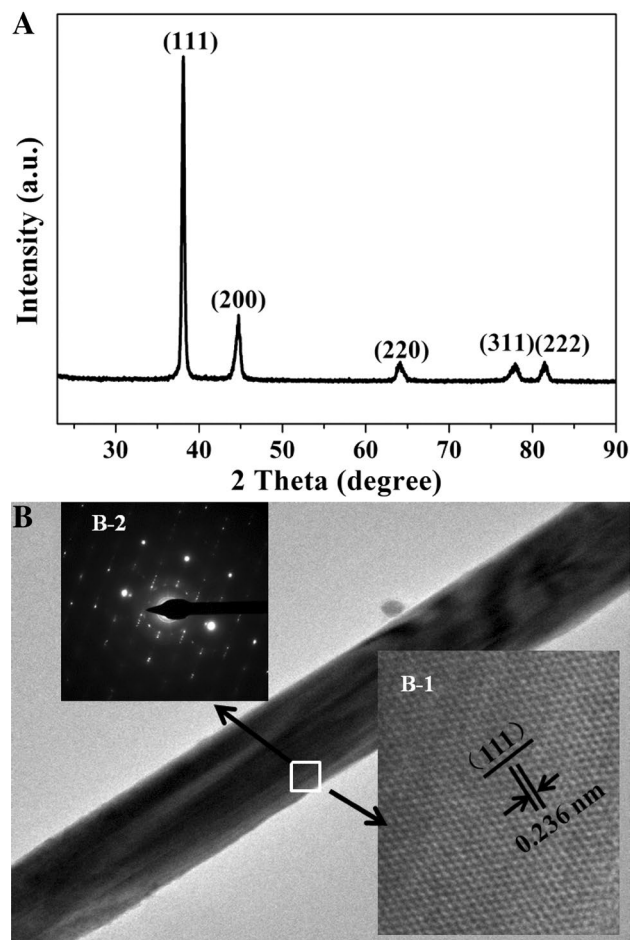


**Fig. 2** a XRD pattern of AgNWs. b HR-TEM image of a typical AgNWs. The estimated d values of 0.236 nm (b-1) and the selected-area electron diffraction (SAED) patterns of AgNWs (b-2)

length and smaller diameters has many advantages in the applications of conductive film, so it desirable to apply in flexible transparent conductor films. Finally, the AgNWs@PVA transparent conductive film fabricated on plastic substrates (polyethyleneterephthalate, PET) exhibited a low sheet resistance and high stability of its electrical conductivities against the repeated bending test.

## 2 Experimental procedure

### 2.1 Materials and methods

$\text{FeCl}_3$ ,  $\text{CuCl}_2 \cdot 2\text{H}_2\text{O}$ , NaBr, EG,  $\text{AgNO}_3$ , PVP and PVA were of analytical grade were used as received without further purification. For a typical synthesis of AgNWs, a one-pot reaction was employed to mix all compounds and solvents. Briefly, 0.40 g of PVP ( $M_w \approx 1,300,000$ ) was first added to 25 mL of EG and completely dissolved using

magnetic stirring at 443 K. To achieve ultra-high aspect ratio AgNWs, 1 mL of 10 mM  $\text{CuCl}_2 \cdot 2\text{H}_2\text{O}$  and 4 mM  $\text{FeCl}_3$  were added into to the PVP solution. Subsequently, 10 mL of  $\text{AgNO}_3$  (0.35 M) and  $\text{NaBr}$  (2 mM) solution was added into the mixture and stirred for 40 min at 443 K and then cooled down to room temperature. The products were adequately washed with de-ionized water and acetone. In our synthesis, the amount of  $\text{AgNO}_3$ , PVP,  $\text{NaBr}$  and EG were set as 0.5943, 0.40, 0.0021 g and 35 mL, respectively, unless stated especially, and the  $\text{Cu}^{2+}/\text{Fe}^{3+}$  molar ratios was changed as 5:1, 5:2, 5:3 and 5:5. The as-prepared AgNWs were dispersed again in DI water solution, in which PVA binder was pre-dissolved. The PVA binder improved the dispersion and adhesion of AgNWs on the PET substrate. This formulation was coated onto the pre-cleaned PET substrate using a bar-coater. A uniform AgNWs@PVA film was coated immediately behind the moving bar-coater. Subsequently, the coated AgNWs@PVA film was placed it in the oven cured for about 1 h at 100 °C to give AgNWs@PVA conductive thin film.

## 2.2 Characterization

The composition of the as-prepared product was examined using powder X-ray diffraction. The morphologies

of the products were observed using a TESCAN S3400N scanning electron microscope. The sheet resistance was measured using the standard four-point probe technique. The optical transmission spectrum was measured using a double-beam spectrophotometer (SHI-MADZU, UV-3101) with air as reference.

## 3 Results and discussion

Figure 1 shows a typical synthesized AgNWs under the  $\text{Cu}^{2+}/\text{Fe}^{3+}$  molar ratio of 5:2. Figure 1a, b was the SEM images of AgNWs, nanowires with diameter of 30 nm and length of 120  $\mu\text{m}$  can be recognized in the images. Figure 1a shows the SEM image of AgNWs and illustrates that the reaction product is mainly composed of large amount of nanowires with a mean length 120  $\mu\text{m}$ . Figure 1b is the high-magnification SEM image, which reveals that the nanowires are uniform in diameter with a mean diameter of 30 nm. The aspect ratio of the obtained AgNWs is about ~4000. Additionally, based on an appropriate adjustment of the reactions, the average diameter of AgNWs is about 30 nm while the yield of one-dimensional nanostructures in the products is as much as 98%. Additionally, this synthesis can be readily scaled up to

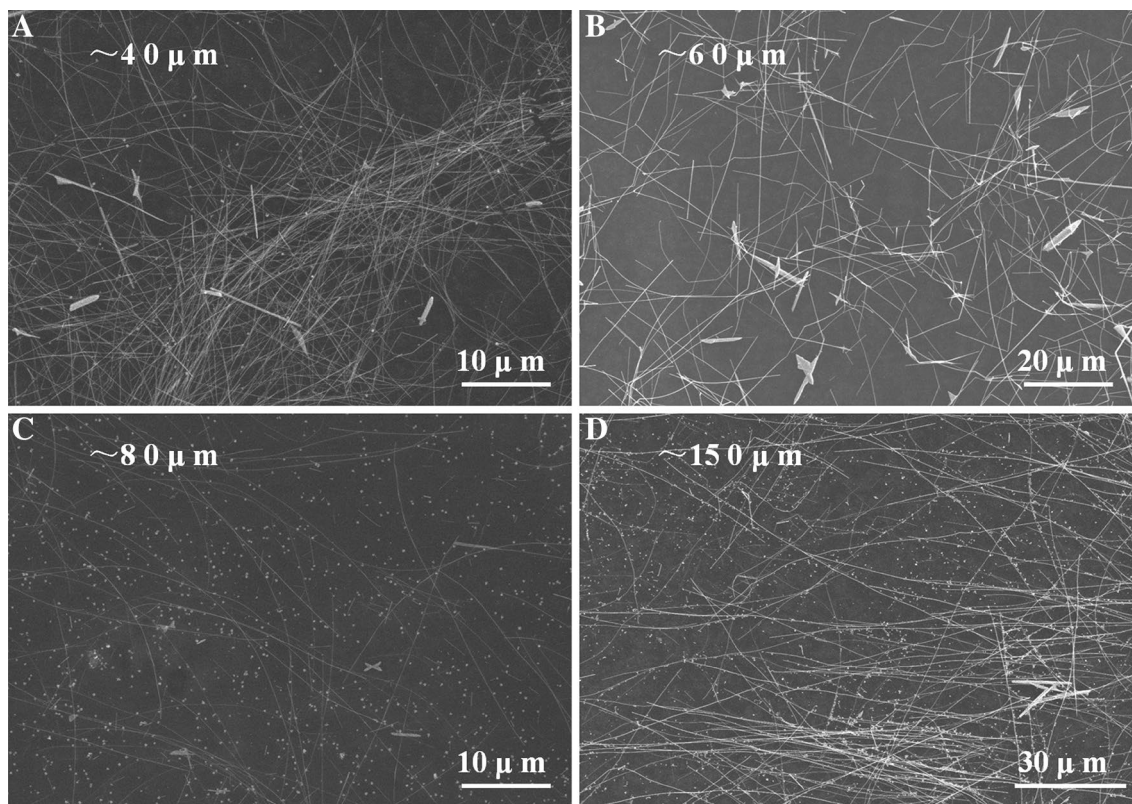


**Fig. 3** SEM images of AgNWs prepared with a  $\text{Cu}^{2+}$  ions concentration of **a** 3 mM  $\text{CuCl}_2 \cdot 2\text{H}_2\text{O}$ , **b** 5, **c** 7, and **d** 10 mM

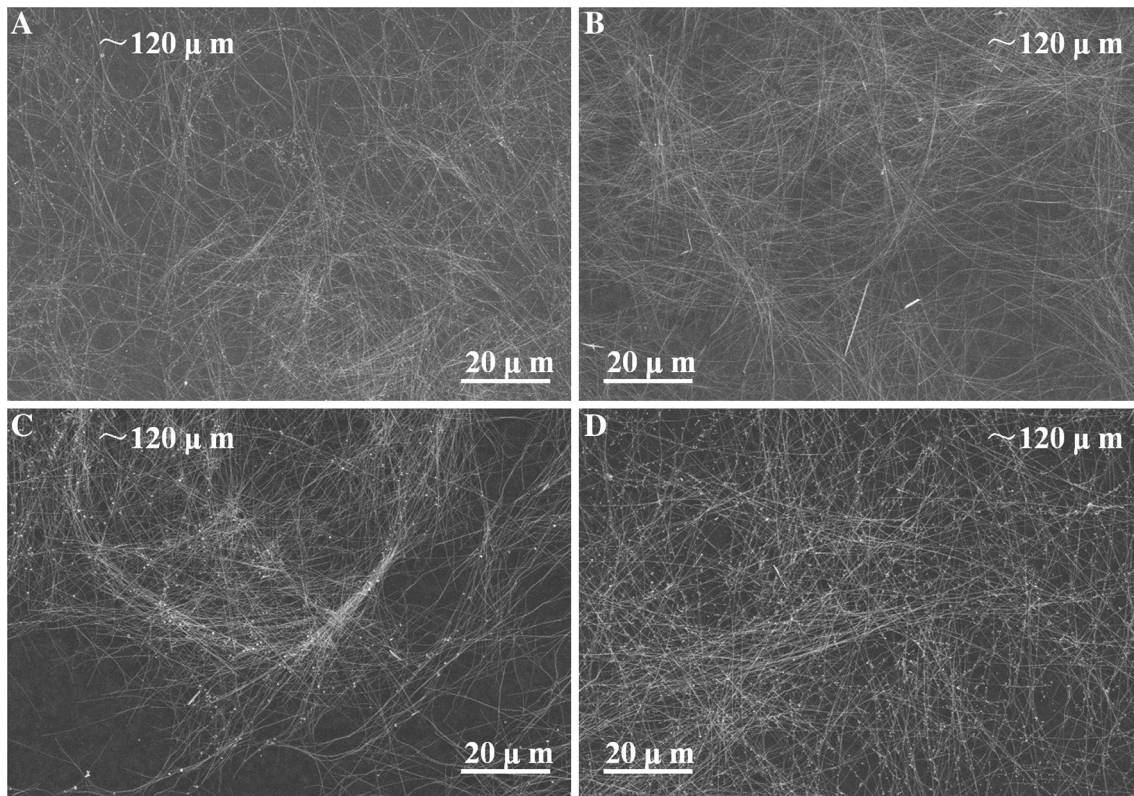


**Fig. 4** SEM images of AgNWs synthesized at different  $\text{Cu}^{2+}/\text{Fe}^{3+}$  molar ratio: **a** 5:1; **b** 5:2; **c** 5:3; **d** 5:5

produce a large quantity of AgNWs and each pot can provide more than 50 g of AgNWs (as shown as Fig. 1b-1).

Figure 2a depicts the XRD pattern of the uniform AgNWs. All the diffraction peaks can be indexed to the (111), (200), (220), (311) and (222) planes of pure face-centered-cubic silver crystal, which is consistent with the standard value according to JCPDS Card No. 04-0783 [22]. The XRD result shows that the high crystalline quality of the AgNWs could be obtained through this facile route. No impurities are detected, indicating the formation of highly pure AgNWs. Figure 2b shows the HRTEM image of a typical AgNWs, revealing the nanowires to be highly crystalline with estimated of 0.236 nm for adjacent lattice planes corresponds to the (111) planes of face-centred silver [Fig. 2b (b-1)] [18]. Figure 2b (b-2) is the SAED pattern taken from the body of AgNWs. Figure 2b (b-2) is the ferent electron diffraction pattern of silver nanowires with a fivefold twinned crystal structure, and the site tested corresponds to the body part indicated by the square in Fig. 2b. This pattern typically consists of two sets of spots corresponding to either side of the nanowires, which represents the characteristic reflection twins in an fcc metal and displays the reflection symmetry about the (111)-type plane [18].

Figure 3 shows the SEM images of AgNWs under different concentration of  $\text{Cu}^{2+}$ . First, we increase the concentration of  $\text{Cu}^{2+}$  in the fabrication, as shown in Fig. 3. It is found through experiments that the by-product of Ag particles increases with the increasing of  $\text{Cu}^{2+}$  concentration. However, with the concentration of  $\text{Cu}^{2+}$  increasing to 5 mM, the average length of AgNWs was improved from 40  $\mu\text{m}$  in 3 mM to 60  $\mu\text{m}$  in 5 mM as shown in Fig. 3a, b. Continuously increasing the concentration of  $\text{Cu}^{2+}$ , the products contain a large number of Ag particles. It is worth mention that the length of AgNWs has increased sharply, to roughly 80  $\mu\text{m}$  in 7 mM and 150  $\mu\text{m}$  in 10 mM as shown in Fig. 3c, d, which was superior to normal polyol method [21]. It was found that the AgNWs length changed according to the concentration of  $\text{Cu}^{2+}$ . The results indicated that, the high concentration of  $\text{Cu}^{2+}$  is favorable for improving the formation of ultra-long AgNWs.

But as we all know, it is not enough to obtain AgNWs with the right dimensions and high aspect ratio; they must also be highly pure and uncontaminated by the presence of nanoparticles. Because nanoparticle impurities dramatically decrease the electrical conductivity and transparency of nanowires networks [23, 24]. In previous reports, the  $\text{Cu}^{2+}/\text{Fe}^{3+}$  molar ratios is seldom considered during the formation and evolution process of uniform AgNWs. In this

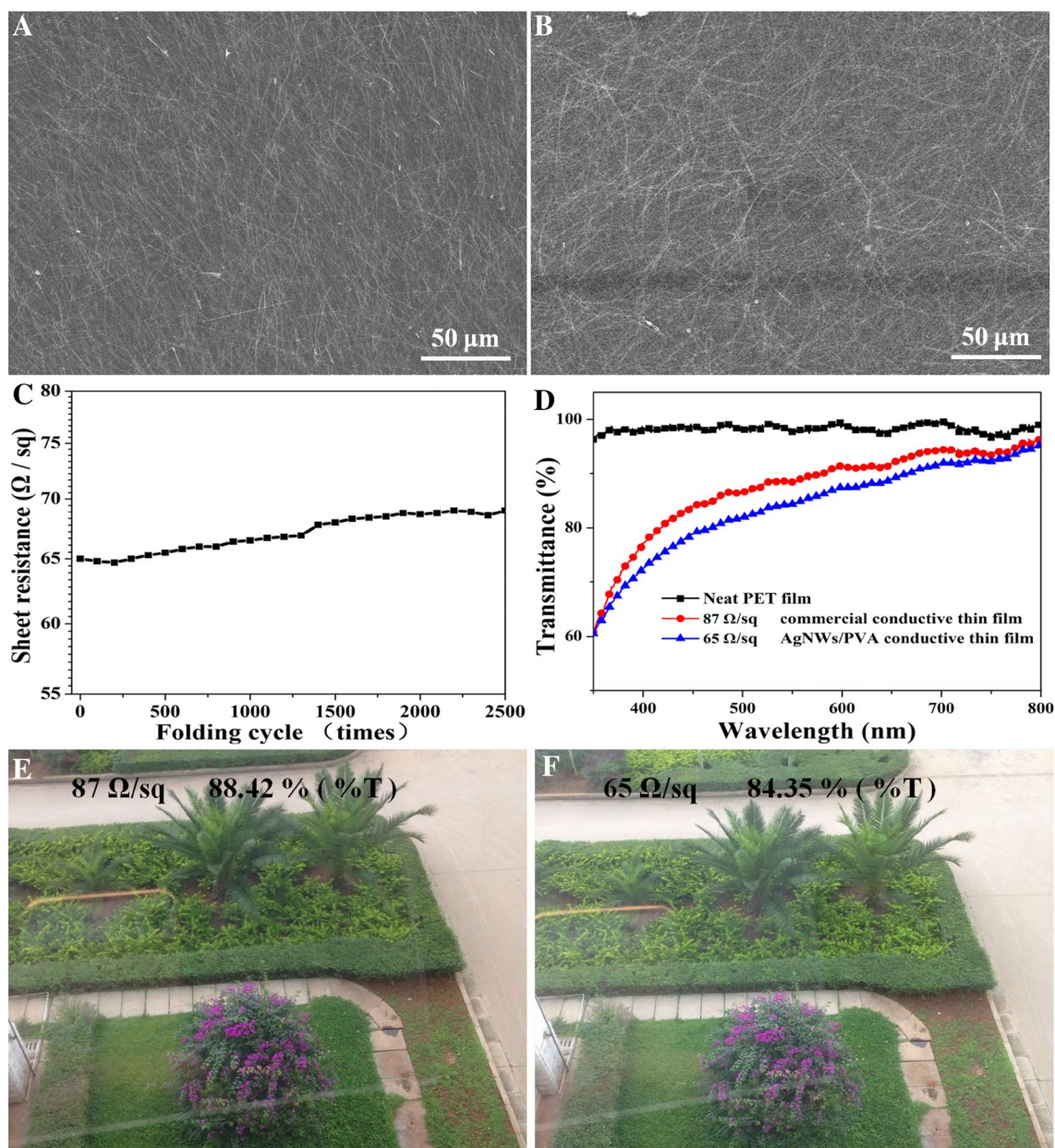


**Fig. 5** **a** SEM image of AgNWs@PVA conductive thin film surface; **b** SEM image of the commercial conductive thin film surface; **c** sheet resistance changes of AgNWs@PVA conductive thin film during 3000 cycles of folding; **d** transmittance spectra of neat PET film and

conductive thin films with specified sheet resistance; optical photographs of the commercial conductive thin film (**e**) and AgNWs@PVA conductive thin film (**f**)

study, the uniformity of AgNWs was studied by changing the  $\text{Cu}^{2+}/\text{Fe}^{3+}$  molar ratios due to the  $\text{Fe}^{3+}$  could affect the uniformity and morphology of AgNWs. Figure 4 shows SEM images of AgNWs obtained at different  $\text{Cu}^{2+}/\text{Fe}^{3+}$  molar ratios. As seen from Fig. 4a, b, uniform AgNWs with diameter of 30 nm and ultra-high aspect ratio up to 4000 were synthesized under different  $\text{Cu}^{2+}/\text{Fe}^{3+}$  molar ratios (5:1 and 5:2). Further, decreasing the molar ratios of  $\text{Cu}^{2+}/\text{Fe}^{3+}$  to 5:3 and 5:5 resulted in many more nanoparticles

in the reaction products (Fig. 4c, d). Experimental results presented in Fig. 4 suggest that the better uniformity upon addition of  $\text{Fe}^{3+}$  and iron ions facilitated the growth of multiply twinned seeds to form nanowires by removing oxygen from the surface of twinned seeds and preventing their dissolution by oxidative etching [25]. Curiously, when the concentration of  $\text{Fe}^{3+}$  was increased to 5:3 and 5:5 (Fig. 4c, d), besides obtaining ultra-long AgNWs, a small amount of silver nanoparticles such as spheres and nanorods

appeared. The significant differences proved that  $\text{Fe}^{3+}$  was an important uniformity-controlling factor in the synthesis of AgNWs with better uniformity and ultra-high aspect ratio up to 4000. However, with excess amounts of  $\text{Fe}^{3+}$ , spherical nanoparticles, polyhedral and nanorods were obtained as main products, and almost no nanowires could be viewed. More detailed mechanism investigation on how the  $\text{Cu}^{2+}$  and  $\text{Fe}^{3+}$  cooperative control the growth process of the AgNWs with better uniformity and ultra-high aspect ratio is now in progress.

The conductive thin film was fabricated by coating an AgNWs-PVA solution on PET substrate and subsequently placed it in the oven cured for about 1 h at  $100^\circ\text{C}$  to give AgNWs@PVA conductive thin film. Surface morphology of the AgNWs@PVA conductive thin film on PET substrate was image by SEM as shown in Fig. 5a. Additionally, the connections between the crossed AgNWs were mainly due to Van der Waals interactions between AgNWs and post mechanical rubbing. The AgNWs were stacked closely, with no spaces between them, and thus form the conducting network and exhibit better electrical conductivity. Figure 5b is the surface morphology of the conductive thin film which is already commercial applications. However, there has been no obvious distinction between the two kinds of conductive thin films (Fig. 5a, b). Moreover, the conductivity and transmittance of the synthesized AgNWs@PVA is the most important thing we care about, which decides whether the nanocomposite can be used as conductor or not. Electrical measurements of hybrid conductive films were conducted using the four-probe technique. The AgNWs@PVA conductive thin film is highly flexible, thus sheet resistance measured after folding-relaxation cycles is shown in Fig. 5c. In the first 1200 folding cycles, no degradation is observed. Thereafter, the resistance slowly increases with folding cycles, and after 3000 folding cycles, the sheet resistance has increased from 65 to 69  $\Omega/\text{sq}$ . The net increase is only 6.15%. Based upon the results in this work, it is believed that the AgNWs@PVA conductive thin film should be a promising conductive material in electronics industry, which requires high electrical conductivity and foldability.

Figure 5d shows the transmittance spectra of the neat PET substrate, commercial conductive thin film and AgNWs@PVA conductive thin film. The transmittance at 550 nm is 88.42% (commercial conductive thin film, Fig. 5e) and 84.35% (AgNWs@PVA conductive thin film, Fig. 5f) for films with sheet resistances of 87 and 65  $\Omega/\text{sq}$ , respectively. Figure 5e, f shows photographs of two representative conductive thin films. All of the conductive thin films are transparent so that our back garden is clearly visible through the conductive thin films. It found no noted differences between AgNWs@PVA conductive thin film and commercial conductive thin film with regard

to transmittance, as shown in Fig. 5e, f. Moreover, the sheet resistance of AgNWs@PVA conductive thin film decreases for the using of AgNWs with ultra-high aspect ratio up to 4000 compare to the commercial conductive thin film. It is noteworthy that the sheet resistance of the AgNWs@PVA conductive thin film is about 25% smaller than the one of the commercial conductive thin film. Therefore, due to the excellent bending property, low resistance and high degree of transparency, the AgNWs@PVA conductive thin film has a great potential to serve as a flexible electrode in many devices.

## 4 Conclusion

In summary, large-scale (over 50 g per pot), uniform AgNWs with diameter of 30 nm and ultra-high aspect ratio (over 4000) were obtained by simply controlling  $\text{Cu}^{2+}/\text{Fe}^{3+}$  molar ratios in the reaction process. In contrast, the AgNWs prepared via the addition of  $\text{Cu}^{2+}$  alone or lower  $\text{Cu}^{2+}/\text{Fe}^{3+}$  molar ratios contained more nanoparticles such as spheres, polyhedral and nanorods. Additionally, flexible ultra-high aspect ratio AgNWs-based conductor thin film was fabricated using one-step strategy method. The above methods improved the production efficiency of ultra-high aspect ratio AgNWs and could be applied to high performance flexible transparent conductor films (TCFs); thus having major commercial implications.

**Acknowledgements** This work is supported by the National Natural Science Foundation of China (Grant No. 61540074), the Basic Applied Research Foundation of Yunnan Province, China (Grant No. 2016FD126) and the fund of the State Key Laboratory of Advanced Technologies for Comprehensive Utilization of Platinum Metals (No. SKL-SPM-201521).

## References

1. B. Li, S. Ye, I.E. Stewart, S. Alvarez, B.J. Wiley, *Nano. Lett.* **15**, 6722–6726 (2015)
2. K.-S. Kim, B.-G. Park, K.-H. Jung, S.-B. Jung, J.-W. Kim, *J. Mater. Sci.* **26**, 8644–8651 (2015)
3. L.J. Andrés, M.F. Menéndez, D. Gómez, A.L. Martínez, N. Bristow, J.P. Kettle et al., *Nanotechnology* **26**, 265201 (2015)
4. Y. Mao, C. Wang, H. Yang, *Mater. Lett.* **150**, 101–104 (2015)
5. X. Peng, F. Tan, W. Wang, X. Qiu, F. Sun, X. Qiao et al., *J. Mater. Sci.* **25**, 1149–1155 (2014)
6. S. Ye, A.R. Rathmell, Z. Chen, I.E. Stewart, B.J. Wiley, *Adv. Mater.* **26**, 6670–6687 (2014)
7. M. Zubair, N. Duraisamy, K. Choi, M. Hyun, *J. Mater. Sci.* **25**, 1033–1039 (2014)
8. S. Sorel, P.E. Lyons, S. De, J.C. Dickerson, J.N. Coleman, *Nanotechnology* **23**, 185201–185209 (2012)
9. J. Lee, P. Lee, H.B. Lee, S. Hong, I. Lee, J. Yeo et al., *Adv. Funct. Mater.* **23**, 4171–4176 (2013)
10. R.M. Mutiso, M.C. Sherrott, A.R. Rathmell, B.J. Wiley, K.I. Winey, *ACS Nano* **7**, 7654–7663 (2013)

11. S.M. Bergin, Y.-H. Chen, A.R. Rathmell, P. Charbonneau, Z.-Y. Li, B.J. Wiley, *Nanoscale* **4**, 1996–2004 (2012)
12. Y.H. Wang, N.N. Xiong, Z.L. Li, H. Xie, J.Z. Liu, J. Dong et al., *J. Mater. Sci.* **26**, 7927–7935 (2015)
13. Z.L. Li, H. Xie, D. Jun, Y.H. Wang, X.Y. Wang, J.Z. Li, *J. Mater. Sci.* **26**, 6532–6538 (2015)
14. Y. Tang, W. He, S. Wang, Z. Tao, L. Cheng, *J. Mater. Sci.* **25**, 2929–2933 (2014)
15. Y. Mao, C. Wang, H. Yang, *Mater. Lett.* **142**, 102–105 (2015)
16. J. Jiu, T. Araki, J. Wang, M. Nogi, T. Sugahara, S. Nagao et al., *J. Mater. Chem. A* **2**, 6326–6330 (2014)
17. Y. Song, M. Wang, X. Zhang, J. Wu, T. Zhang, *Nanoscale Res. Lett.* **9**, 1–8 (2014)
18. S. Liu, B. Sun, J.-G. Li, J. Chen, *CrystEngComm* **16**, 244–251 (2014)
19. C. Jia, P. Yang, A. Zhang, *Mater. Chem. Phys.* **143**, 794–800 (2014)
20. A. Amirjani, P. Marashi, D.H. Fatmehsari, *Coll. Surf. A* **444**, 33–39 (2014)
21. S. Wang, Y. Tian, S. Ding, Y. Huang, *Mater. Lett.* **172**, 175–178 (2016)
22. K.L. Kelly, E. Coronado, L.L. Zhao, G.C. Schatz, *J. Phys. Chem. B* **107**, 668–677 (2003)
23. A. Tao, P. Sinsersuksakul, P. Yang, *Angew. Chem. Int. Ed.* **45**, 4597–4601 (2006)
24. K.C. Pradel, K. Sohn, J. Huang, *Angew. Chem. Int. Ed.* **50**, 3412–3416 (2011)
25. B. Wiley, Y. Sun, Y. Xia, *Langmuir* **21**, 8077–8080 (2005)